ACCADEMIA NAZIONALE DEI LINCEI

CONVEGNO

GEODESY AND PLANETARY SCIENCES: A GEODETIC CONFERENCE FOR GEODESY AND ASTRONOMY AT THE ACCADEMIA DEI LINCEI

13 MAGGIO 2025

A B S T R A C T

Comitato ordinatore: Mattia CRESPI (Linceo, Università la Sapienza), Francesca MATTEUCCI (Lincea, Università di Trieste), Fernando SANSÒ (Linceo, Politecnico di Milano, coordinatore).

PROGRAMMA

Geodesy is one of the oldest "modern" sciences, born together with Mechanics and Astronomy between XVII and XVIII century. We recall that the first empirical proof of Newton's law, namely the decrease of the gravitational attraction with the squared inverse of the distance, has been of geodetic character, based on a model of the Earth with spherical layers of constant mass density. This is the same law controlling the motion of bodies in the Solar system, if not of the whole Universe, which however requires more advanced physical theories, like General relativity, Astrophysics, to account for its evolution. On the same time the positioning on the Earth surface was taking advantage of the direction of the vertical on the celestial sphere; just think of ancient navigation instruments like the astrolabe. These models and technologies are today superseded by modern tools for the observation of the Earth in particular from the full deployment of e.m. connections between ground stations and satellites. For instance the determination of the dynamics of Earth satellites, under the complicated gravitational pull of the earth gravity field, is nowadays controlled by laser ranging as well as radio-wave phase observations like those of the Global Navigation System (GNSS). The positioning of points on the Earth and the navigation on its surface are again matter of using GNSS observations. Not to be mentioned the possibility of sounding the Earth surface with optical, radar or other e.m. waves at different wavelengths, to derive its physical state, e.g. temperature, humidity of the soil or wind forcing of the ocean. Exactly the same, or similar, methods are used for instance to follow and control planetary space missions, or to determine the presence and state of atmospheres on planets, as well as of their surface. This seems a valid reason for the Accademia dei Lincei to devote one of the recurring Geodetic Days to the exploration of the interface between the two sister sciences: Geodesy and Astronomy.

Martedì 13 maggio

9.30 Saluto della Presidenza dell'Accademia Nazionale dei Lincei

9.40 Fernando SANSÒ (Linceo, Politecnico di Milano), Giuseppe BIANCO (ASI): *Theory and Practice of Terrestrial and Celestial Reference Systems*

10.20 Luciano IESS (Sapienza Università di Roma): *The navigation in the planetary system*

10.50 David LUCCHESI (IAPS-INAF): *The scientific challenges of Earth satellites*

11.20 Coffee break

11.50 Mattia CRESPI (Linceo, Sapienza Università di Roma, Scuola Superiore di Studi Avanzati): *Positioning on the Earth*

12.20 Cosimo STALLO (ESA): *Positioning on the Moon*

12.50 Intervallo

14.00 Francesco BERRILLI (Linceo, Università Tor Vergata): *Solar activity and space weather*

14.30 Elvira ASTAFYEVA (IPGP-Paris): *Sounding of the Earth Ionosphere*

15.00 Cinzia ZUFFADA (NASA Jet Propulsion Laboratory): *The exploration of atmospheres and surfaces of the planets*

15.30 Coffee break

16.00 Stefano FEDERICO (CNR): *Sounding of the Earth atmosphere*

16.30 Paola MALANOTTE (Lincea, MIT): *Monitoring the global ocean circulation and properties*

17.00 Riccardo LANARI (CNR): *Sounding of the deforming solid Earth surface*

ROMA – PALAZZO CORSINI- VIA DELLA LUNGARA, 10
Segreteria del convegno: convegni@lincei.it – http://www.lincei.it

Tutte le informazioni per partecipare al convegno sono disponibili su:
https://www.lincei.it/it/manifestazioni/geodesy-and-planetary-sciences

Per partecipare al convegno è necessaria l'iscrizione online
Fino alle ore 10 è possibile l'accesso anche da Lungotevere della Farnesina, 10
I lavori potranno essere seguiti dal pubblico anche in streaming

L'attestato di partecipazione al convegno viene rilasciato esclusivamente a seguito di partecipazione in presenza fisica e deve essere richiesto al personale preposto in anticamera nello stesso giorno di svolgimento del convegno

Sistema di Riferimento

Per i fisici spesso il “sistema di riferimento” non è altro che il banco su cui montare un esperimento.

Per i geodeti e gli astronomi che devono posizionare punti lontani tra loro, il concetto è centrale e va definito con precisione, tanto che ad esempio la IAG ne ha fatto il nucleo della propria attività scientifica.

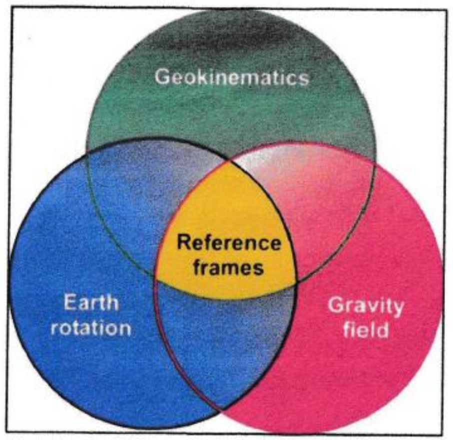

Semplifichiamo il problema.

Studiamo un problema della stessa natura ma con meno variabili.

1. Π (poliedro) corpo geometrico con N vertici che voglio descrivere per mezzo di coordinate $\boldsymbol{x}^T \equiv [\boldsymbol{x}_1^T \ldots \boldsymbol{x}_N^T]$; dim $\boldsymbol{x} = 3N$
2. i punti sono connessi tra loro solo con misure (es. distanze)
3. le misure sono modellate da leggi fisiche note (incluso il loro ambito di applicazione)
4. le misure Y_i contengono sempre errori: $Y_i = y_i + \varepsilon_i (i = 1 \ldots N)$, cioè la ripetizione delle misure porta a valori diversi; y_i, le osservabili, sono valori medi di Y_i ed a loro si applicano le leggi fisiche; ε_i sono interpretati come discrepanze stocastiche e descritti come estrazione da variabili casuali a media nulla.

Esempio

Π è fatto di N punti materiali nel vuoto, senza movimento (o con basse velocità); la velocità della luce c è costante; le misure sono tutte le distanze Y_{ik}, tra P_i e P_k; le leggi che governano le misure sono galileiane, cioè esiste un tempo assoluto (tutti gli orologi possono essere sincronizzati); la geometria è euclidea; le deviazioni dall'ambito galileiano, ad esempio relativistiche, possono essere calcolate a priori ed applicate direttamente alle misure, riportandoci al modello precedente.

Ridondanza

Se M_0 sono le misure (ad esempio distanze Y_{ik}) che fissano rigidamente Π ed M sono le misure effettuate, ci saranno $r = M - M_0$ misure ridondanti.
Per ogni misura ridondante esiste una relazione geometrica tra le osservabili $\{Y_{ik}\}$.
Ad esempio: se per 3 punti (Q_1, Q_2, Q_3) misuriamo le distanze reciproche (d_{12}, d_{13}, d_{23}), possiamo fissare rigidamente il triangolo dei 3 punti. Se poi ogni altro punto $P_k (k = 4 \dots L)$ è raggiunto da 3 distanze da (Q_1, Q_2, Q_3), allora il punto P_k risulterà fissato nello spazio. Dunque Π è fissato rigidamente da $M_0 = 3 + 3L$ misure; ogni altra misura di distanza tra i P_k sarà ridondante e porterà ad una relazione tra le osservabili.

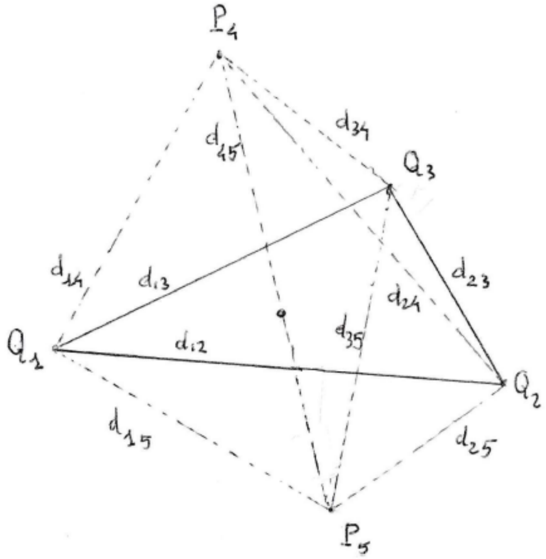

Le osservabili

$d_{12}d_{13}d_{14}d_{15}, d_{23}d_{24}d_{25}, d_{34}d_{35}$

fissano Π; l'osservabile d_{45} è ridondante ed esisterà una relazione
$d_{45} = f(d_{ik})\ \ (i,k) \neq (4,5).$

Scrivere le equazioni (di condizione) per le misure ridondanti è possibile ma complesso; per questo si preferisce descrivere Π attraverso le coordinate dei punti;
$N = L + 3,$ numero di coordinate $3N = 3L + 9$
Π <u>isodeterminato</u>
$r = 0\ ;\ M_0 - 3N = (3L+3) - (3L+9) = -6$ g.d.l. non determinati

Π sovradeterminato ad esempio con tutte le distanza; la ridondanza è
(distanza tra i P_k)

$$r = M - M_0 = \frac{L(L-1)}{2} = \frac{(N-3)(N-4)}{2} > 0 \text{ per } N \geq 5 \ .$$

Tuttavia il numero delle $\{Y_{ik}\}$ indipendenti, cioè non legate da relazioni, continua ad essere M_0 e quindi ci sono sempre 6 gradi di libertà non determinabii dalle misure; i 6 g.d.l. corrispondono esattamente ai parametri di una rototraslazione che trasformano un poliedro Π con certe coordinate $\boldsymbol{x}$, in un altro Π' con coordinate $\boldsymbol{x}'$ che però lasciano invarianti le distanze tra punti in R^3.

In astratto: la varietà $\mathcal{A}$ nello spazio delle osservabili R^M ha dimensione $\boxed{\dim \mathcal{A} = M - r}$; ogni punto di $\mathcal{A}$, $\widehat{\boldsymbol{y}}$, corrisponde ad un poliedro $\widehat{\Pi}$ di forma defnita che posso rappresentare come voglio in un sistema cartesiano $(\boldsymbol{O}, \boldsymbol{e}_1, \boldsymbol{e}_2, \boldsymbol{e}_3)$; ogni altro poliedro congruente è rappresentato dallo stesso $\widehat{\boldsymbol{y}}$; $\mathcal{A}$ può anche avere una rappresentazione parametrica

$$\widehat{\boldsymbol{y}} = g(\boldsymbol{x}) ;$$

se $\boldsymbol{x}$ è il vettore di tutte le coordinate di tutti i punti in $(\boldsymbol{O}, \boldsymbol{e}_1, \boldsymbol{e}_2, \boldsymbol{e}_3)$ la corrispondenza non è biunivoca; cioè esistono molti $\widehat{\boldsymbol{x}}(t)$ tali che

$$\widehat{\boldsymbol{y}} = \boldsymbol{g}[\widehat{\boldsymbol{x}}(\boldsymbol{t})]; \ \forall \boldsymbol{t} \in R^p ;$$

l'indice p rappresenta la sovraparametrizzazione e nel nostro caso è pari a 6, come i g.d.l. della rototranslazione.

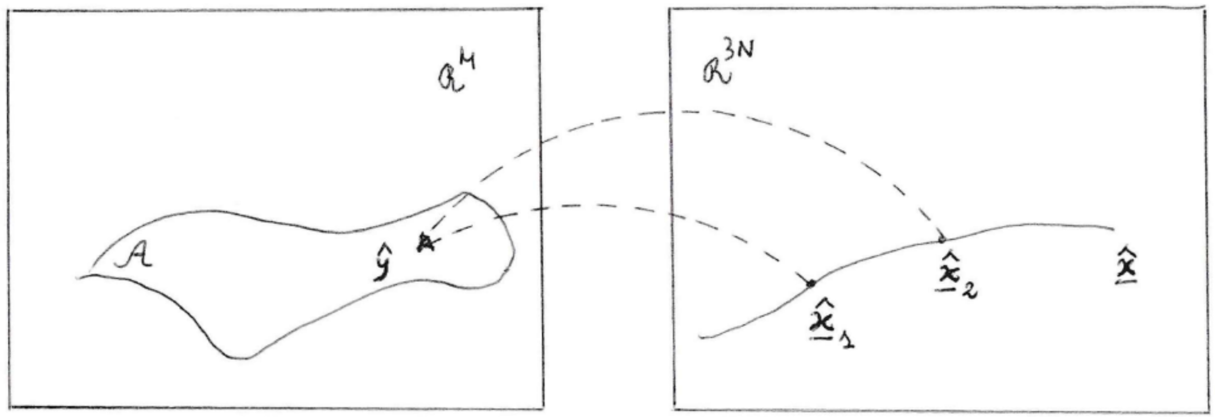

$$\widehat{\boldsymbol{y}} = \boldsymbol{g}[\widehat{\boldsymbol{x}}(\boldsymbol{t})] \quad \forall \boldsymbol{t} \in R^6$$

Nota: siccome $\widehat{\boldsymbol{y}}$ è costante rispetto a $\boldsymbol{t}$, vale $0 = \frac{\partial \boldsymbol{g}}{\partial \boldsymbol{x}} \cdot \frac{\partial \boldsymbol{x}}{\partial \boldsymbol{t}}$

Poichè $\boldsymbol{y}_0 = \boldsymbol{y} + \varepsilon$, a causa di $\varepsilon, \boldsymbol{y}_0 \notin \mathcal{A}$; cioè $\boldsymbol{y}_0$ non è compatibile col fatto che le osservabili si riferiscano a un poliedro Π; occorre trovare uno stimatore $\widehat{\boldsymbol{y}} \in \mathcal{A}$ che sia statisticamente vicino a $\boldsymbol{y}_0$; questo è dato di solito dal metodo dei minimi quadrati (m.q.);

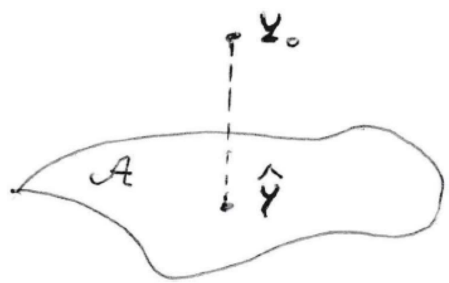

$$
\begin{aligned}
\widehat{Y}_{\text{m.q.}} &= \arg\min_{\widehat{\boldsymbol{y}} \in \mathcal{A}} |\boldsymbol{y}_0 - \widehat{\boldsymbol{y}}|^2_{\varepsilon} = \\
&= \arg\min_{\widehat{\boldsymbol{y}} \in \mathcal{A}} (\boldsymbol{y}_0 - \widehat{\boldsymbol{y}})^T C_{\varepsilon}^{-1} (\boldsymbol{y}_0 - \widehat{\boldsymbol{y}})
\end{aligned}
$$

l'uso di C_{ε}^{-1} è dovuto al teorema di Gauss–Markov–Aitken per il caso lineare.

Teorema

Se le equazioni per $\widehat{y}$ sono lineari

$$B\widehat{\boldsymbol{y}} = \boldsymbol{b} \Leftrightarrow \widehat{\boldsymbol{y}} \in \mathcal{A}$$

tra tutti gli stimatori lineari corretti $\widehat{\boldsymbol{y}} = L\boldsymbol{y}_0 + \boldsymbol{\ell}$ quelli di m.q.

$$\widehat{\boldsymbol{y}}_{\mathrm{m.q.}} = \boldsymbol{Y}_0 + C_\varepsilon B^T (BC_\varepsilon B^T)^{-1} (\boldsymbol{b} - B\boldsymbol{Y}_0)$$

è quello di minima dispersione di $\widehat{\boldsymbol{y}}(TrC_{\widehat{y}} = \min)$. Cioè la forma di $\widehat{\Pi}$ (legato agli errori) è meno variabile.
Nota: naturalmente le equazioni di condizione per $\widehat{\boldsymbol{y}}$ sono non lineari, ma possono essere linearizzate.

Definizione 1 di R.F.

L'esistenza, almeno in linea di principio, di $\widehat{\boldsymbol{y}}_{\mathrm{m.q}}$ ci permette di dare una prima definizione di R.F.
Definizione 1: R.F. è il poliedro $\widehat{\Pi}$ definito dal vettore $\widehat{\boldsymbol{y}}_{\mathrm{m.q}}$.
Se voglio rappresentare $\widehat{\boldsymbol{y}}$ per coordinate $\boldsymbol{x}$, allora devo invertire la relazione $\widehat{\boldsymbol{y}} = \boldsymbol{g}(\boldsymbol{x})$; poichè questa ha molte soluzioni $\widehat{\boldsymbol{x}}(\boldsymbol{t})$, devo imporre su $\boldsymbol{x}$ 6 condizioni. Le più semplici sono

$$\begin{cases} x_1 = y_1 = z_1 = 0 & \Rightarrow \quad \text{origine in } P_1 \\ y_2 = z_2 = 0 & \Rightarrow \quad \text{asse } X \text{ per } P_1 \text{ e } P_2 \\ z_3 = 0 & \Rightarrow \quad \text{piano } (X, Y) \text{ per } P_3. \end{cases}$$

Le condizioni poste bloccano ogni traslazione e rotazione del sistema di coordinate, quindi si possono ricavare $(\widehat{x}_2, \widehat{x}_3, \widehat{y}_3, \widehat{x}_4, \widehat{y}_4, \widehat{z}_4 \ldots)$ in base al principio dei m.q.

$$\widehat{\boldsymbol{x}} = \arg\min_{\boldsymbol{x}} |\boldsymbol{y}_0 - \boldsymbol{g}(\boldsymbol{x})|^2_{\varepsilon}$$
$$(x_1 = y_1 = z_1 = y_2 = z_2 = z_3 = 0)$$

trovando una soluzione “particolare” $\widehat{\widehat{\boldsymbol{x}}}$, cioè il poliedro $\widehat{\Pi}$ inquadrato nel sistema cartesiano in cui i vettori $\boldsymbol{x}_1, \boldsymbol{x}_2, \boldsymbol{x}_3$ soddisfano le condizioni poste.

Nota: senza condizioni le soluzioni $\widehat{\boldsymbol{x}}$ non si possono trovare algebricamente perché le equazioni di minimo non sono indipendenti

$$- \quad \left(\frac{\partial \boldsymbol{g}}{\partial \boldsymbol{x}}\right)^T C_\varepsilon^{-1}(Y_0 - g(\boldsymbol{x})) = 0 \ ;$$

$$\left(\frac{\partial \boldsymbol{x}}{\partial \boldsymbol{t}}\right)^T \left(\frac{\partial \boldsymbol{g}}{\partial \boldsymbol{x}}\right)^T C_\varepsilon^{-1}(Y_0 - g(\boldsymbol{x})) \equiv 0 \text{ perché } \frac{\partial \boldsymbol{g}}{\partial \boldsymbol{x}} \frac{\partial \boldsymbol{x}}{\partial \boldsymbol{t}} \equiv 0 \ .$$

Una volta nota la soluzione particolare $\widehat{\widehat{\boldsymbol{x}}}$ si possono trovare tutti i vettori $\widehat{\boldsymbol{x}}(t)$ per la fibra che contiene $\widehat{\widehat{\boldsymbol{x}}}$, per mezzo di una rototraslazione, cioè

$$\widehat{\boldsymbol{x}}_i(t) = \boldsymbol{\tau} + U\widehat{\widehat{\boldsymbol{x}}}_i \quad \boldsymbol{\tau} = \text{ traslazione}, U = \text{rotazione :}$$

si pone perciò il problema di ottimizzare $(\boldsymbol{\tau}, U)$ in modo che il poliedro stimato sia il meno possibile influenzato dagli errori, ovvero

$$TrC_{\widehat{\boldsymbol{x}}(t)} = \sum_{i=1}^{N} TrC_{\boldsymbol{x}_i} = \min \; ;$$

linearizzando le equazioni si trova una soluzione eplicita di m.q (vedi F. Sansò, S. Dermanis - Rendiconti Lincei v29–2018).

Esempio Elementare

In R^1, $\Pi \equiv \{a, b\}$, $y = D_{ab}$, $\boldsymbol{x} = \begin{vmatrix} x_a \\ x_b \end{vmatrix}$.
Il sistema di riferimento è realizzato dall'origine O di X g.d.l. non determinabili 1; $r \equiv 0$

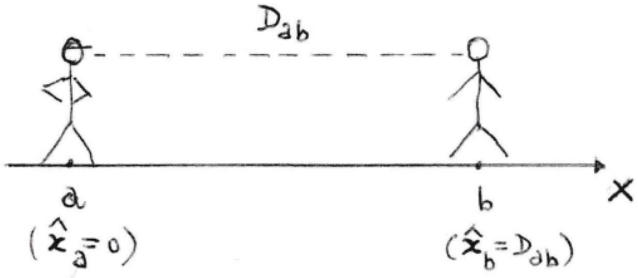

$$\boxed{Y = D_{ab} + \varepsilon = x_b - x_a + \varepsilon}$$

Se a è prepotente, porre $a \equiv 0$, cioè

$$x_a = 0 \Rightarrow \widehat{\widehat{\Pi}} = \{\widehat{x}_a = 0, \widehat{x}_b = D_{ab}\}$$

Variabilità di $\widehat{\widehat{\Pi}}$; $\quad \sigma_a^2 + \sigma_b^2 = 0 + \sigma_\varepsilon^2$

Esempio Elementare

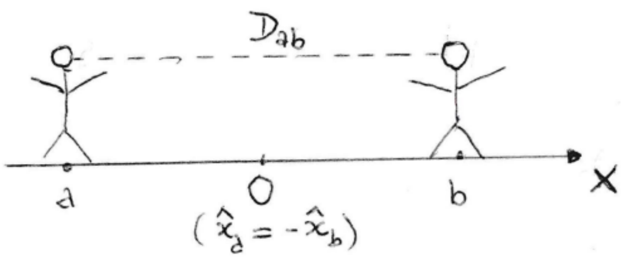

$$\widehat{\Pi} = \left\{ \widehat{x}_a = -\frac{D_{ab}}{2} \ , \ \widehat{\boldsymbol{x}}_b = \frac{D_{ab}}{2} \right\}$$

Variabilità di $\widehat{\Pi}$

$$\sigma_a^2 + \sigma_b^2 = \frac{\sigma_\varepsilon^2}{4} + \frac{\sigma_\varepsilon^2}{4} = \frac{1}{2}\sigma_\varepsilon^2 \ !$$

Se a e b si mettono d'accordo.
$0 =$ punto di mezzo tra a e b

Si dimostra che questa è la soluzione ottimale.

Vari tipi di vincoli (condizioni sulle coordinate) si possono trovare generalizzando l'esempio monodimensionale.
Ad esempio, si possono imporre le condizioni

$$\sum_{1=1}^{N} x_i = \sum_{i=1}^{N} y_i = \sum_{i=1}^{N} z_i = 0 \; ; \quad \text{blocca la traslazione}$$

$$\sum_{1=1}^{N} x_i y_i = \sum_{i=1}^{N} x_i z_i = \sum_{i=1}^{N} y_i z_i = 0 \; ; \quad \text{blocca la traslazione}$$

In ogni caso i poliedri stimati con opportune condizioni, in numero di 6, sono tra loro congruent, cioè rototraslati.

Definizione 2 di R.F.

Definizione 2: un R.F. è un poliedro $\widehat{\Pi}$ corrispondente a coordinate cartesiane $\widehat{\boldsymbol{x}}$, soddisfacenti a un qualche gruppo di condizioni (6 per il caso statico) che bloccano la possibilità di rototraslare.

È chiaro che se si ripetono le stesse misure su Π, gli errori di misura variano e quindi anche la forma di $\widehat{\Pi}$ e le sue coordinate $\widehat{\boldsymbol{x}}$ variano; cioè un R.F. è per sua natura stocastico. Se si fanno N misure e si fa $N \to +\infty$, per il teorema centrale della statistica il poliedro tende a quello vero

$$\widehat{\Pi} \to \Pi \ \text{ cioè } \ \widehat{\boldsymbol{x}} \to \boldsymbol{x} \ ;$$

il sistema di coordinate cartesiane $(\boldsymbol{O}, \boldsymbol{e}_1, \boldsymbol{e}_2, \boldsymbol{e}_3)$ può allora essere visto come la terna identificata dal corpo ideale invertendo le condizioni che si sono usate per $\widehat{\boldsymbol{x}}$.
È questo per definizione il R.S., cioè il limite per $N \to +\infty$ dei R.F.

Naturalmente la situazione reale anche solo per il R.F. terrestre è molto più complicata; in primo luogo, i punti hanno 6 g.d.l. ciascuno, 3 coordinate (x, y, z) e le loro variazioni temporali $(\dot{x}, \dot{y}, \dot{z})$ che in modello ancora semplificato risultano costanti, inoltre si usa il tracking da satellite come distanze per definire $\widehat{\Pi}$ e $\widehat{\boldsymbol{x}}$; ciò comporta di introdurre la dinamica del satellite e quindi la rotazione terrestre ed il suo campo di gravità nelle equazioni d'osservazione della distanze e poi...

questi temi saranno affrontati nel prossimo intervento.

The navigation in the planetary system

Luciano IESS (Sapienza Università di Roma)

Positioning and navigation in the near-Earth environment—both on the ground and in space—has become almost effortless, thanks to the advanced infrastructure provided by global navigation satellite systems, pioneered by the U.S. Department of Defense's Global Positioning System. However, deep space navigation presents a much more complex challenge, especially when high-accuracy orbit determination and positioning are required. Navigation between and around planets relies primarily on radio links at microwave frequencies, which are established between ground antennas and deep space probes. These radio links not only maintain the vital connection with mission controllers and scientists, but they also provide crucial data to determine the spacecraft's position and trajectory.

In Earth navigation, whether terrestrial, maritime or aerial, measurements of angles, distances, and velocities were key. Deep space navigation uses similar measurements—specifically, range, range rate, and very long baseline interferometry (or delta-differential one-way ranging, ΔDOR, in the navigation jargon). These quantities, ultimately derived from time measurements, emphasize the importance of precise clocks and frequency standards. State-of-the-art radio systems can measure range (i.e. travel time of a pseudo-noise code from the ground antenna to the spacecraft and back) with an accuracy of a few centimeters across the entire solar system, as demonstrated by the mission BepiColombo mission of the European Space Agency (ESA). Similarly, high-precision range rate data (essentially radial velocity) were recorded by NASA's Deep Space Network during the Cassini spacecraft's cruise to Saturn, achieving an accuracy of 1×10^{-6} m/s over 1000 s intervals. In navigation terms, VLBI is often referred to as delta-differential one-way ranging (ΔDOR). All of these measurements ultimately depend on precise timekeeping, underscoring the importance of accurate clocks and frequency standards. Modern radio systems can measure range (the travel time of a pseudo-noise code sent from a ground antenna to a spacecraft and back) with an accuracy of just a few centimeters across the entire solar system, as demonstrated by the European Space Agency's BepiColombo mission. The best range rate data (essentially, radial velocity) was obtained by NASA's Cassini spacecraft during its cruise to Saturn. Under optimal conditions, NASA's Deep Space Network measured a range rate of 1×10^{-6} m/s, averaged over 1000-second intervals. Additionally, the angular position of a spacecraft relative to quasars that define the International Celestial Reference Frame (ICRF) can be determined with remarkable accuracy—around one nanoradian—by observing the spacecraft and a quasar from two widely separated ground antennas. Optical imaging and altimetry can also assist in navigation under special circumstances. Although laser links may complement radio tracking in the future, they are unlikely to replace it in the foreseeable future.

While high-quality observational data are essential for precise navigation, they are not sufficient on their own. As in any dynamical system, a spacecraft's orbit is determined by matching measured quantities with those predicted by a dynamical model of the solar system. This model relies on our knowledge of gravitational laws, the orbits of solar system bodies, and their gravity fields. Non-gravitational accelerations—such as those from solar radiation pressure—are often difficult to model or measure and add complexity to spacecraft dynamics. Currently, the non-geodesic motion of the spacecraft is the main limitation to very precise orbit determination and positioning of space probes. High-sensitivity, unbiased, and stable accelerometers would provide an invaluable improvement. Deep space tracking systems are now so precise that even intrinsecally random phenomena, like variations in solar irradiance or solar wind pressure, can be detected in range and range rate data—such as those from BepiColombo's cruise phase—requiring the use of stochastic dynamical models.

Space missions not only rely on the laws of physics and knowledge of solar system dynamics for navigation, but they also contribute significantly to advancing our understanding of fundamental physics and planetary geodesy. For instance, the precision of Newton-Einstein gravitational laws is confirmed by space missions through radio tracking. Probes like the Viking landers and Cassini spacecraft have provided excellent and still unsurpassed experimental confirmations of general relativity. Spacecraft have have been inserted in orbit around all terrestrial planets, the Moon, and the outer planets Jupiter and Saturn. In 2033, the European Space Agency's JUICE spacecraft will enter a low, circular orbit around Ganymede, the largest moon in the solar system. Radio tracking of these orbiting spacecraft has significantly improved our knowledge of solar system dynamics, allowing the mission's navigation teams to rely on highly accurate planetary ephemerides when planning and executing orbital maneuvers. For example, the accuracy of the astronomical unit (the yardstick

of the solar system) has greatly improved over time, from 17th-century angular measurements to modern radar bouncing and radio tracking.
The free motion of space probes is almost entirely governed by gravity. Unsurprisingly, the navigation infrastructure has been widely exploited to measure the gravity field of planets and satellites, giving an extraordinary boost to planetary geodesy and geophysics. Gravity is the only force that interacts with everything and cannot be blocked by anything. While measuring the external gravity field of a planet does not directly reveal its internal mass distribution, these measurements provide crucial insights into a planet's interior structure, which is key to understanding its formation. For example, gravity data have revealed hidden oceans beneath the icy surfaces of moons like Titan and Enceladus, and have provided the depth of the zonal winds on Jupiter and Saturn. These discoveries illustrate the synergy between space navigation, planetary geodesy, and fundamental physics—where science and engineering work together.
The telecommunication infrastructure provided by the main space agencies (such as NASA's Deep Space Network and ESA's ESTRACK) has supported both mission operations and scientific investigations, leading to a wealth of scientific discoveries. However, many regions of our solar system remain unexplored, and numerous questions remain unanswered. New missions and advanced tools will be essential for further progress. Optimistically, as human missions to the solar system become more feasible, the advancements in precise navigation and planetary geodesy will play a crucial role in making these missions a reality.

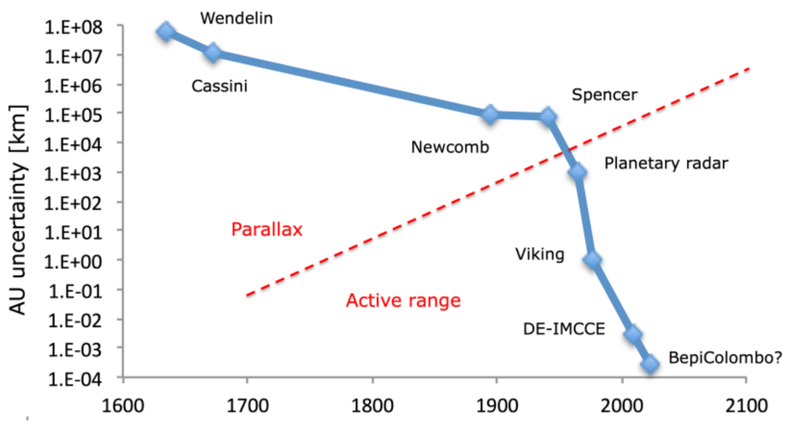

Fig. 1. The uncertainty in the knowledge of the astronomical unit, from Wendelin and Cassini measurements to modern ephemerides enabled by active radio tracking.

The scientific challenges of Earth satellites

David LUCCHESI (IAPS-INAF)

The circumterrestrial space is today characterized by the presence of a very high number of artificial satellites, from relatively low orbits of a few hundred km from the Earth's surface, up to orbits a few tens of thousands of km away. Depending on use, the orbits can be circular or elliptical, and with different inclinations, from equatorial to polar. Orbital motion can be direct (anticlockwise), in the direction of the Earth's rotation, or retrograde (clockwise), in the direction opposite to the Earth's rotation. Artificial satellites have a variety of very different uses, ranging from weather forecasting to communications and broadcasting, from navigation to Earth observation, from military uses to scientific research, to name just a few.
Artificial satellites can be divided into active and passive. The former, the majority, are characterized by the presence of motors for maneuvering, antennas for telecommunications with the ground or for their tracking and by the presence on board of a large variety of sensors to be used for many types of in situ measurements, related to the Earth itself, to the atmosphere that surrounds it, to its gravity and magnetic fields, or to the Sun and the solar system and the cosmos in general.
Unlike the former, passive satellites do not have any particular instruments on board and they do not have engines or antennas. They are generally covered with retro-reflecting mirrors, or sometimes transponders, to determine their orbit with great precision. Most geodetic satellites belong to this type of satellite, used for the geophysical study of the Earth and for space geodesy in general.
A very outstanding example of these kind of passive satellites is LAGEOS (LAgeos GEOdynamics Satellite), launched by NASA in 1976. This geodynamic satellite has provided and still provides a significant

contribution in determining the low-degree spherical harmonics of the Earth's gravitational field, in the determination of the Earth's center of mass, the so-called geocenter, and the Earth's polar motion, to name just a few of the main applications of its precise orbit determination (POD). This POD is achieved through the precise SLR (Satellite Laser Ranging) technique which exploits the measurement of the round-trip time of flight of short laser pulses emitted from a network of ground stations, down to the millimeter level of precision. The ILRS (International Laser Ranging Service) supports laser ranging measurements to geodetic, remote sensing, navigation, and experimental satellites equipped with retroreflector arrays as well as to reflectors on the Moon. The ILRS coordinates activities for the international network of SLR and LLR (Lunar Laser Ranging) stations. The network represents a global consortium of permanent and mobile field stations that range to ILRS approved targets for science and engineering applications.
Since the mid-1990s, the LAGEOS satellite, together with its twin LAGEOS II, launched by ASI and NASA in 1992, have been successfully used to test gravitation and fundamental physics, in the weak-field and slow-motion (WFSM) limit of Einstein's linearized theory of General Relativity (GR).
These series of measurements, which exploit the high precision of the SLR technique together with a concomitant development of refined models for the main gravitational and non-gravitational perturbations acting on these satellites, have allowed to verify the predictions of GR on the orbit of these geodetic satellites and to compare them with the corresponding predictions of other alternative theories of gravitation. These measurements have allowed us to place significant constraints on several theories of gravitation, both metric, such as GR, and non-metric, the latter theories not assuming the validity of Einstein's Equivalence Principle. Some of these results are related to the precise and accurate measurement of the main relativistic precessions acting on these satellites, linked to the existence of the Gravitoelectric and Gravitomagnetic fields of GR.
The presentation focuses on the applications and results of the two LAGEOS satellites and other geodetic satellites in the fields of fundamental physics and gravitation.

Positioning on the Earth

Mattia CRESPI (Linceo, Sapienza Università di Roma, Scuola Superiore di Studi Avanzati)

Positioning on the Earth is a broad topic involving a variety of technologies and methods. This contribution focuses on outdoor positioning based on true satellite signals on direct line-of-sight. Outdoor positioning based on signals from quasars (Very Long Baseline Interferometry - VLBI) and from ground stations (Satellite and Lunar Laser Ranging - SLR and LLR, Doppler Orbitography and Radiopositioning Integrated by Satellite - DORIS), which is relevant to realize the global reference frame, and positioning based on pseudolites, on classical geodetic surveying techniques and on diverse indoor techniques is not here discussed.
With this limitation, the status and the modernization perspectives of positioning based both on Global Navigation Satellite Systems (GNSS) (US GPS, Russian GLONASS, Chinese Beidou and EU Galileo), on regional navigation satellite systems (Indian NavIC and Japanese QZSS) and on new constellations of Low Earth Orbit (LEO) satellites are addressed; in this frame, positioning is intended in a broader sense, considering not only positions, but also other kinematic parameters (velocities, accelerations).
These positioning systems include diTerently featured satellites, placed on diTerent orbits at diTerent altitudes (LEO, Medium Earth Orbit (MEO), Geostationary Earth Orbit (GEO), Geosynchronous Orbit (GSO) and Inclined Geosynchronous Orbit (IGSO)), transmitting diTerent signals (partially on common frequencies within the L-band), but the positioning principle and the underlying fundamental technology is just unique, what allows to jointly use these systems in an interoperable way.
The positioning principle is trivial: user-to-satellite distances are measured, satellite positions are considered as known (they bring the reference frame to the user), user position on the Earth is estimated from distances geometric intersection in space.
What is definitely less trivial is to actually measure user-to-satellite distances, to provide satellite positions, and to define what is the user position on the Earth.

Starting from user-to-satellite distance measurements, they are basically time measurements on the complex signals broadcasted by satellites on diTerent frequencies in L-band (wavelengths within 20 to 30 cm). Measurements can be performed on codes or carrier phases: in the first case, using codes, accuracy is lower (few decimeters), but realtime measurements are feasible, enabling real-time positioning; in the second, using carrier phases, a much higher accuracy (up to tenths of millimeters) is achievable, but realtime measurements are impossible, due to the intrinsic ambiguity of carrier phases, which cannot be solved using time measurements on codes yet, due to their still insuTicient accuracy. Noteworthy, also near real-time measurements are tricky, due to the dependence of ambiguity parameters estimability on the satellite geometric configuration variation, which is too slow for present global/regional positioning systems mainly based on MEO satellites. Also, user-to-satellite distance measurements are impacted by three additional problems: both using codes or carrier phases, measurements are performed in 1-way mode, that is using two clocks, one on satellite (transmission time) the other at user (reception time), which are intrinsically asynchronized; in addition, diTerent positioning systems refer to diTerent time references, which are mutually asynchronous too; the propagation time is impacted by atmospheric (ionosphere and troposphere) behavior, which must be accounted for to determine the Euclidean distance, scaling the corrected propagation time with the speed of light.

Coming to user position on the Earth, it is dependent on the periodic and secular motions of the Earth surface (mainly solid tides and tectonics), which must be accounted for to define the user position at a certain nominal epoch.

Finally, satellite positions themselves depend, on one hand, on distance measurements to satellites from "special users" (ground permanent stations), whose positions on the Earth are considered as known and are updated continuously, in a sort of circular fashion forth and back between ground permanent stations and satellites.

All in all, positioning based on global/regional satellite positioning systems depends on time measurements, based on asynchronous clocks, with respect to diTerent time references and on solid and fluid Earth models; also, the type of signal used (codes or carrier phases) to perform time measurements impacts two key features of satellite positioning: accuracy and real-time/oT-line availability.

The future goal of satellite positioning is therefore to pursue high accuracy in real time, and three objectives are delineated: (i) to further improve time measurements on codes, therefore improving real-time user-to-satellite distance measurement accuracy (Figure 1); (ii) to solve for carrier phase ambiguity in real time, dependent both on real-time user-tosatellite distance measurement accuracy and on faster satellite geometric configuration variation, which justify the launch of new LEO constellations (Figure 2); (iii) to improve solid and fluid Earth models.

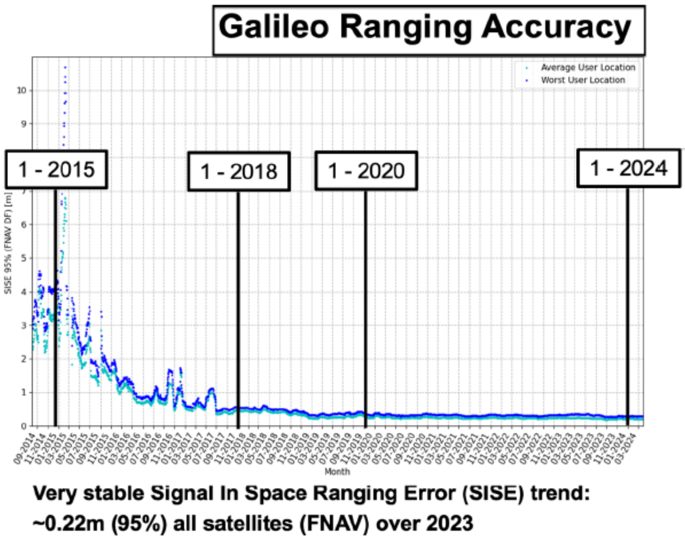

Figure 1 - Galileo ranging accuracy evolution
(Credits: M. Falcone, ESA NAV Directorate - *30 years of IGS*, Bern, 1-5 July 2024)

Figure 2 - GNSS multilayers overall constallation
(Credits: M. Falcone, ESA NAV Directorate - *30 years of IGS*, Bern, 1-5 July 2024)

Positioning on the Moon

Cosimo STALLO (ESA)

In recent years, lunar exploration has regained momentum, driven by technological advancements and international collaborations. Governments and private companies aim to establish a sustainable presence, harness lunar resources, and prepare for future Mars missions. NASA's Artemis program, alongside China's and other nations' efforts, marks a new era of space exploration.

The European Space Agency has launched its program called Moonlight Lunar Communications and Navigation Services (LCNS), an initiative to create a satellite constellation orbiting the Moon for communications and navigation services. With over 400 planned lunar missions by space agencies and private companies in the next two decades, this program marks a significant step towards sustainable lunar exploration and the development of a lunar economy.

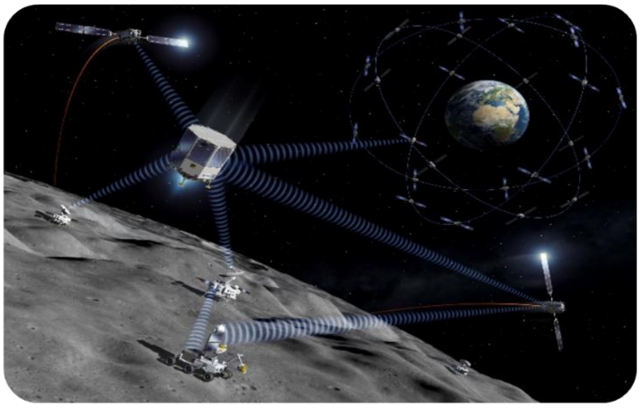

This programme will enable precise, autonomous landings and surface mobility, while facilitating high-speed, low-latency communication and data transfer between Earth and the Moon.
Moonlight will consist of five satellites – four for navigation and one for communications – connected to Earth via three dedicated ground stations, creating a data network spanning up to 400 000 km. The satellites will be strategically positioned to prioritise coverage of the lunar South Pole.

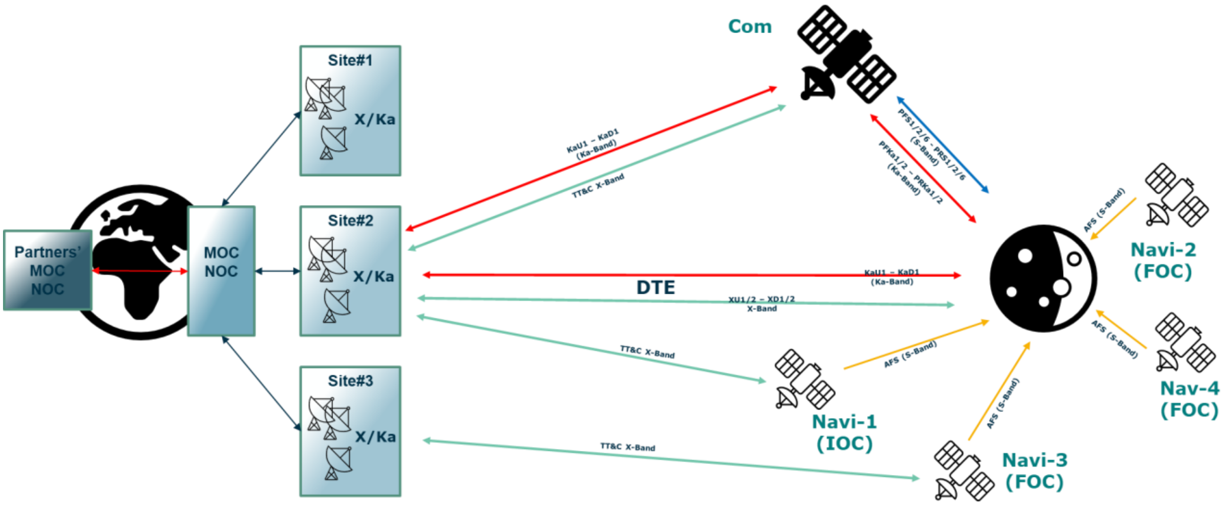

Mission Architecture Concept

This presentation will focus on the E2E navigation chain overview of Moonlight and describe its design, expected performances and how it will support future landing and surface missions.

Solar activity and space weather

Francesco BERRILLI (Linceo, Università Tor Vergata)

The Sun exhibits long-term, impulsive and cyclical variations in activity, most notably the 11-year Schwabe cycle, driven by its evolution and changes in its global and local magnetic field. This solar variability influences a range of phenomena, including fluctuations in total and spectral irradiance, the occurrence of solar flares and coronal mass ejections, and variations in the solar wind and energetic particle acceleration. These solar events significantly affect the physical conditions of interplanetary space, including the space environment surrounding Earth, creating the conditions for space weather or space climate, depending on the time scales involved.
The regular and irregular variability of solar activity exerts a significant influence on the chemical reactions and physical processes within the Earth's atmospheric system, resulting in

substantial modulations of the structure and evolution of the ionosphere and thermosphere. The Earth's upper atmosphere absorbs solar radiation, leading to heating, dissociation, and ionization. The ionosphere primarily forms through the ionization of atmospheric constituents by solar Extreme Ultraviolet (EUV) radiation. Solar EUV exhibits significant variability across various timescales, ranging from minutes (flares) to roughly 27 days (solar rotation) and extending to decadal cycles with different amplitude fluctuations. Shorter wavelengths exhibit greater variability, strongly influencing artificial satellites and the terrestrial atmosphere. This solar activity variability drives substantial changes in the ionosphere, including variations in neutral density (influencing satellite lifetime and satellite/debris de-orbiting), temperature, ion and electron densities and temperatures, neutral winds, and electric fields.

As emphasized in this Conference's introduction, accurately tracking Earth satellites navigating the complex gravitational field of our planet relies heavily on techniques such as laser ranging and radio-wave phase observations, frequently associated with Global Navigation Satellite Systems (GNSS). GNSS is also indispensable for terrestrial positioning and navigation. Crucially, extreme space weather events can severely degrade the stability and performance of second-generation GNSS constellations (Galileo, GPS, GLONASS, BeiDou/Compass) and their augmentation systems, i.e., Satellite Based Augmentation System (SBAS). Furthermore, long-term variations in the space environment (space climate) can induce slow changes in the circumterrestrial environment. These long-term variations may also modify conditions in deep space, potentially influencing human exploration beyond the protective magnetosphere or deep-space missions reliant on high-precision absolute positioning.

Sounding of the Earth Ionosphere

Elvira ASTAFYEVA (IPGP-Paris)

Ionosphere is a region of the Earth’s atmosphere where the concentration of electrically charged particles (i.e., ions and electrons) is enhanced, which is between ~60 and ~1000 km of altitude. The ionosphere is formed by the solar UV ionization. Consequently, it is very sensitive to variations in solar activity. In addition, the ionosphere is sensitive to perturbations in the magnetosphere and the thermosphere, to geophysical phenomena, such as stratospheric warmings, planetary waves, natural hazards (e.g., earthquakes, tsunamis, volcano eruptions) but also to man-made events (e.g., explosions and rocket launches).

Global Navigation Satellite Systems (GNSS) offer a powerful and accessible tool allowing the monitoring of the ionosphere. Due to the dispersive nature of the ionosphere, signals from dual-frequency GNSS receivers make it possible to measure the total electron content (TEC)—the electron density integrated along the raypath from a satellite to a receiver. As of today, the operational GNSS comprise the American Global Positioning System (GPS), Russia's GLONASS, the European Union's Galileo, China's BeiDou, Japan's Quasi-Zenith Satellite System (QZSS), the Indian Regional Navigation Satellite System (IRNSS or NAVIC). Comparatively good coverage of the globe by ground-based GNSS receivers along with long-time continuous measurements have made GNSS widely used to study the ionospheric dynamics and variations.

This presentation will first introduce the basics of the ionosphere and its sounding by GNSS.

Further, it will discuss advantages and unresolved challenges in this sounding technique. Finally, it will present applications of GNSS sounding for studying the ionosphere and the neighboring “spheres”.

The exploration of atmospheres and surfaces of the planets

Cinzia ZUFFADA (NASA Jet Propulsion Laboratory)

Atmospheric science is an important aspect of planetary research, focused on interpreting how the motion and composition of planetary atmospheres can lead to understanding of the origin and evolution of planetary systems. Astronomical bodies retain an atmosphere when their escape velocity is significantly larger than the average molecular velocity of the gases present in the atmosphere.

The atmospheres of the planets in our solar system are remarkably different with hugely variable compositions, temperatures and pressures. Planets such as Venus, Earth, Mars, Jupiter, Saturn, Uranus and Neptune have significant atmospheres. Titan, a moon of Saturn, is known to have a thick atmosphere.

The study of planetary and exoplanetary atmospheres spans a breadth of techniques and disciplines which seek an understanding of the climate, dynamics, and chemistry of atmospheres both in our solar system and beyond. One of the most widely studied aspects is the meteorology of the Martian atmosphere, including carbon-dioxide ice clouds and quantifying the occurrence and development of dust storms on Mars. Another one involves observations of the polar atmosphere of Jupiter.

Planetary surfaces are found in planets, asteroids and natural moons throughout the solar system and surface conditions, temperatures and terrain vary significantly. Besides Earth, humans have only directly explored the surface of the Moon, and indirect observations of a number of other planetary surfaces have been made through fly-bys, orbiters, landers and other surface probes. Surface samples have been collected from the Moon, Mars and asteroids and some have been returned to Earth. Typical instruments used to study planetary surfaces are cameras, imaging spectrometers, mass spectrometers, radars, thermal imagers.

In the US, the priorities for space observations of planetary atmospheres and surfaces are identified in the periodic Decadal Surveys produced by the National Academies of Science by request of the Federal agencies, most recently the Planetary Science and Astrobiology Decadal Survey 2023 and the Solar and Space Physics Decadal Survey 2024. These surveys play a crucial role in shaping NASA's future endeavors, reflecting a broad consensus within the scientific community on the most relevant science questions to be pursued through a robust mission portfolio.

Needed exploration of planetary atmospheres and surfaces combines a range of expertise and skills such as remote sensing data processing and analysis, surface structure modelling, atmospheric science, volcanic modelling and sub-surface geophysical processing and interpretation to allow us to take advantage of the available planetary data to address key questions in planetary science. The talk will review the main research thrusts, highlight key seminal findings and discuss some outstanding questions.

Sounding of the Earth atmosphere

Stefano FEDERICO (CNR)

The Mediterranean area is often struck by severe weather and deep convective events because of the presence of the warm sea, the complex orography of the area and the specific synoptic-scale pressure patterns. This scenario is worsened by the climate change, which is affecting many weather and climate extremes, and the frequency and intensity of heavy-precipitation events have increased in most of the world. Numerical weather prediction (NWP) models are useful tools for predicting adverse weather conditions and to guide responsive actions for mitigating the impact of severe weather. During the last decades, NWP have continuously improved their performance and ability to predict severe weather events thanks to improvement of physical formulation, of data assimilation techniques and of the availability of new observations. Nevertheless, NWPs have well-known difficulties in representing the physical processes at small spatial and temporal scales, which are involved in convective and severe weather events, and research and operational efforts are pursued worldwide to improve the precise prediction of severe weather events.

Errors in NWP models arise from several sources: incomplete knowledge of physical processes, incomplete knowledge of the atmospheric state, physical and numerical parameterisations, and others. Another common problem of NWP-based nowcasting and short-term forecasting is the spinup time because the model needs a few hours to balance the inconsistencies between the initial and boundary conditions to properly reproduce the small-scale dynamic. Data assimilation, especially at the local scale and of local observations is a key factor for reducing this issue and improving the prediction of high-impact weather events. Among local observations, water vapor plays a key role because it regulates humid and energetic exchanges in the atmosphere. Therefore, good knowledge of water vapor distribution in space and time is a fundamental requirement for improving NWP forecasts of convective and severe weather events.

Global navigation satellite system (GNSS – a collective term used to address all global and regional satellite navigation systems, including the Global Positioning System (GPS), Galileo, GLONASS and BeiDou) observations for geodetic and geophysical purposes can provide estimates of the tropospheric delays (generally ZTD – zenith total delay but also STD, i.e. the delay along slant paths), directly connected to the water vapor content in the atmosphere. For this reason, GNSS data have been assimilated into NWP model since three decades. Most of the works focus on the assimilation of GNSS-ZTD or GNSS-PWV (precipitable water vapour) along the zenith direction, nevertheless there are also studies assimilating the delay along slant paths. Compared to other sources of data, GNSS provide a direct estimate of the water vapour content, even if integrated along a path, while for other sources of data, also useful in the forecast of intense convective events (meteorological radar or flashes) the information on the water vapor amount is estimated under some assumptions. Compared to sources of data as radiosoundings, GNSS can provide more observations, both in space and time. This can lead to a longer lasting positive impact of GNSS data assimilation at the local scale (Figure 1).

In this talk, the assimilation of GNSS data into numerical weather prediction models will be reviewed considering experiences worldwide with special focus on the Mediterranean and Italy.

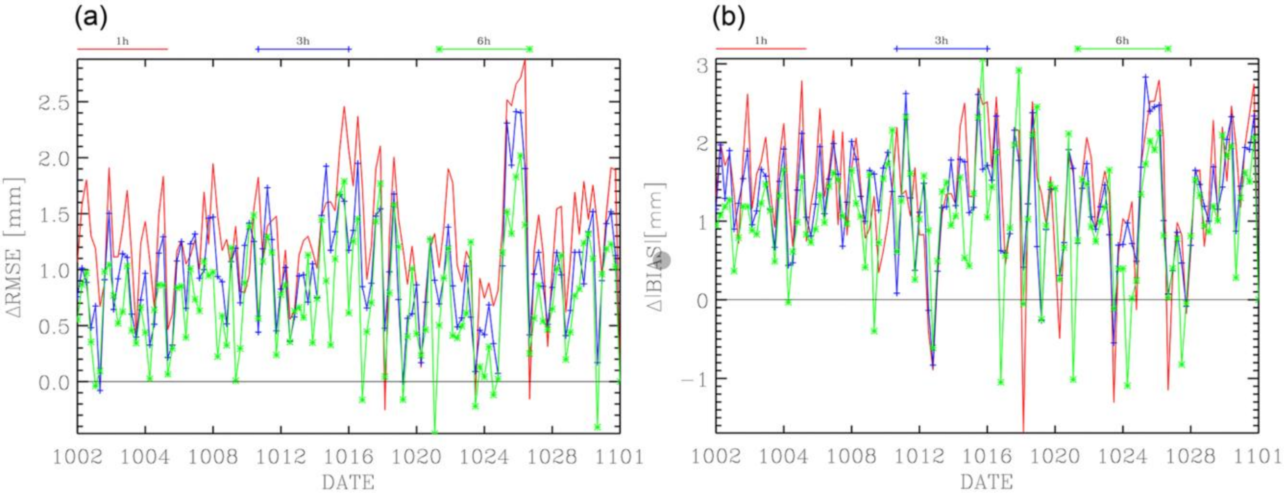

Figure 1: Time series of the differences between PWV-RMSE simulations assimilating (GNSS) and not assimilating (CTRL) GNSS-ZTD observations (a); and of the difference in the absolute value of the BIAS for the CTRL and GNSS simulations (b). The red curve is for the first forecast hour, the blue curve is for the third forecast hour and the green curve is for the sixth forecast hour. The date format is the month followed by the day. From Torcasio et al. (2023).

Reference

Torcasio, R. C., Mascitelli, A., Realini, E., Barindelli, S., Tagliaferro, G., Puca, S., Dietrich, S., and Federico, S.: The impact of global navigation satellite system (GNSS) zenith total delay data assimilation on the short-term precipitable water vapor and precipitation forecast over Italy using the Weather Research and Forecasting (WRF) model, Nat. Hazards Earth Syst. Sci., 23, 3319–3336, https://doi.org/10.5194/nhess-23-3319-2023, 2023.

Monitoring the global ocean circulation and properties
Paola MALANOTTE (Lincea, MIT)

To leading order in the Navier-Stokes equations for fluid motions, the large scale ocean circulation is hydrostatic and geostrophic. Combining the geostrophic equations for the horizontal velocity components and the hydrostatic approximation for pressure, we obtain the thermal wind equations providing the vertical shear of the geostrophic velocities whose integration implies an unknown integration constant representing a horizontal velocity at whatever oceanic level (interior or surface) it may be known. In the classical oceanographic literature of the middle of last century, entire chapters were devoted to the problem of finding the "level of no motion" where velocities were vanishing and from which the thermal wind equations could be integrated providing the complete picture of the large scale oceanic circulation. (Sverdrop, Johnson, Fleming, 1942; Defant, 1961).
From the observational point of view, the problem consists in measuring the large scale interior horizontal density gradients determining the geostrophic shears. Unfortunately, and differently from the atmosphere, the ocean is opaque to electromagnetic radiation which is absorbed roughly in the upper 100 m. at all wavelengths. However, the ocean is transparent to sound which can be transmitted over the entire ocean basins interiors. Perturbations in the travel times in the acoustic rays correspond to perturbations in temperature, density , velocities. The configuration of the first demonstration experiment (Munk et al., 1982) is shown in Fig.1a. Symbols "S" indicate a source of acoustic pulses and "R" a receiver. The horizontal lines schematically show the possible horizontal acoustic pathways going from sources to receivers. Fig. 1b shows the vertical structure of a number of acoustic rays sampling the interior water mass along different vertical paths.

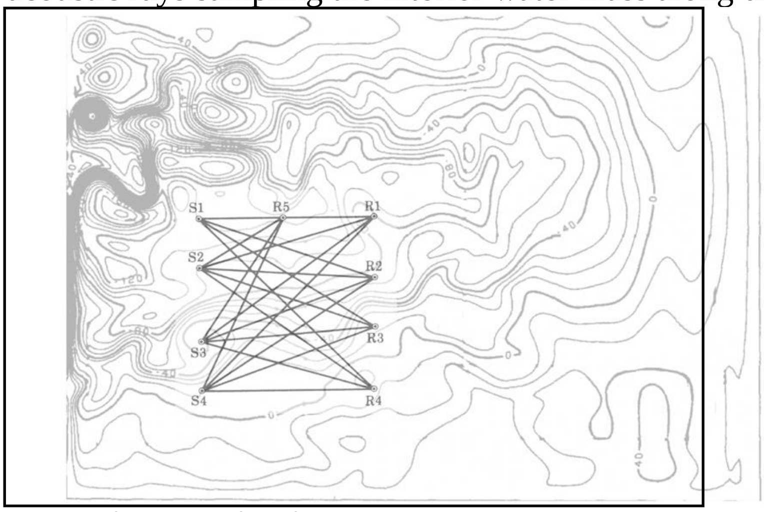

Fig. 1a : Configuration of the first tomography experiment (Malanotte-Rizzoli, 1985)

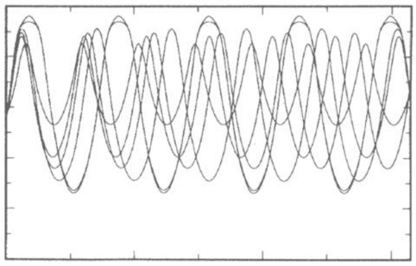

Fig. 1b : Acoustic vertical pathways (Munk et al., 1982)

The early 80s saw also the advent of satellite altimetry through the launching of the TOPEX/Poseidon altimeter, a joint enterprise USA-France. The altimeter was conceived to determine the surface ocean topography and hence the absolute slope of the ocean surface (TOPEX Science Working Group, 1981;European Space Agency, 1980). From the absolute slope the surface geostrophic velocity can be inferred thus providing the reference velocity to close the thermal wind equations. Ocean acoustic tomography and altimetry proved to be the complementary observational tools needed to determine the global ocean circulation at zero order.
The tomographic measure is the average temperature along the acoustic ray paths or the average velocity along two "reciprocal" acoustic paths connecting a couple (S,R). The goal of the first tomography experiments was to "map" the mesoscale eddy field shown in Fig. 1a.Hence the integral measurements must be transformed into piecewise sets of data capable of resolving the mesoscale eddies. This transformation requires the use of rather cumbersome linear inverse theories after having solved the direct problem of tracing (stable) acoustic rays through the interior

temperature fields. Arguably, the optimal application of acoustic tomography is to directly use the average measured data themselves. This motivation led Walter Munk and collaborators to conceive the ATOC experiment : Acoustic Thermometer of Ocean Climate (ATOC Consortium, 1998) whose observational array covering the Pacific ocean interior is shown in Fig. 2a. One of the most important variables to assess the effects of climate warming is ocean temperature (heat content) integrated on the global oceanic basins . Here again satellite altimetry and acoustic tomography proved be the complementary observational tools both providing large-scale averages suitable to detect climate changes. The ATOC array of Fig. 2a is superimposed on the map of the rms sea level anomaly for 4 years of TOPEX/Poseidon measurements, with the acoustic data providing a stable average otherwise impossible to obtain. Fig. 2b shows the heat content change inside the region spanned by the acoustic array for the altimeter-acoustic estimate converted to an equivalent sea surface flux per unit area.

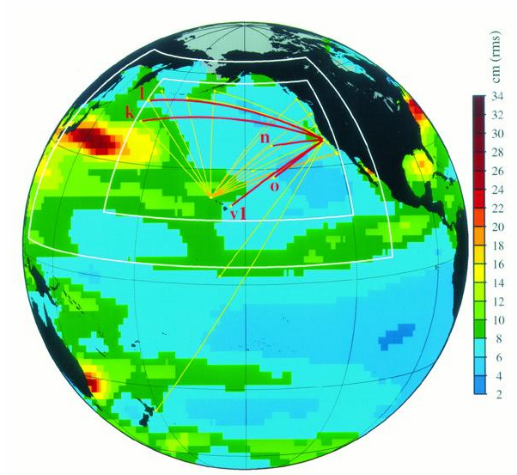

Fig. 2a : The ATOC acoustic array superimposed to a map of the rms sea level anomaly. Red and yellow lines: tomography sections.

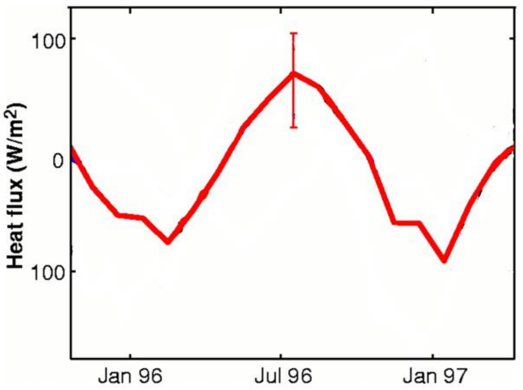

Fig. 2b. Heat content change in the acoustic array

References

ATOC Consortium, *Ocean Climate Change Comparison of Acoustic Tomography, Satellite Altimetry and Modeling*, DOI: 10.1126/science.281.5381.1327, 1998
Defant, A., *Physical Oceanography*, Pergamon Press, Vol. 1, pp.720, 1961
European Space Agency, *Study on satellite radar altimetry in climatological and oceanographic research*, pp. 323, 1980
Malanotte-Rizzoli, P., *J. Phys. Oceanogr*., 15, 416-438, 1985
Munk et al, *Phil. Trans. R. Soc. London*, A, 307, 439-464, 1982
Svedrup, H.U., Johnson, M.W., Fleming, R.H., *The Oceans*, Prentice-Hall Inc., pp. 1060, 1942
TOPEX Science Working Group, *Satellite altimetric measurements of the ocean*, pp. 78, 1981

Sounding of the deforming solid Earth surface

Riccardo LANARI (CNR)

Imaging the Earth surface both day and night and in any atmospheric condition is possible thanks to the Synthetic Aperture Radar (SAR), a sensor which, generally mounted on board satellites or aircrafts (and drones, more recently), operates in the microwave band of the electromagnetic spectrum. In particular, the SAR sensors are equipped with a transmitting and a receiving system through which, by sending appropriate signals, they "illuminate" the areas of interest and record the back-scattered electromagnetic radiations, whose appropriate digital processing allow us to generate high resolution microwave images of the observed zones. An important feature of these radar systems is the possibility of applying the Differential Interferometry SAR (DInSAR) techniques which permit, starting from the phase difference (often referred to as interferogram) of the SAR image pairs acquired at different times, the measurement of ground deformations affecting large areas on Earth, with centimeter (sub-centimeter, in some cases) accuracy.

The DInSAR techniques have undergone a continuous evolution over the last three decades, becoming a very important geodetic tool for effectively sounding the deforming solid Earth surface behavior. In fact, these methods are nowadays widely used both for the study of deformations linked to natural phenomena (seismic, volcanic, hydrogeological), and to anthropic activities (subsoil exploitation, for instance), also allowing the investigation of possible displacements at the scale of single buildings and infrastructures. Moreover, originally designed and applied to investigate single deformation episodes, such as an earthquake or a volcanic eruption, the “original” DInSAR methodology has evolved toward the study of the temporal evolution of the detected displacements thanks to the development of “multi-temporal” (also referred to as “advanced”) DInSAR techniques. Such approaches, which are based on the exploitation of multi-temporal SAR image sequences, relevant to an area of interest, provide helpful information on the spatial and temporal characteristics of the detected deformations, through the generation of displacement time series.

This presentation will start by introducing the basic concepts of the SAR sensors and of the original DInSAR methodology, to then move on to the description of the multi-temporal DInSAR techniques. In particular, to show the capability of these methods to provide helpful information on the spatial and temporal characteristics of the detected deformations, several results obtained from the analysis of the data acquired by the different space-borne SAR sensors, will be presented. This will be done by starting from the first-generation SAR satellites, as in the case of the ERS-1/2 and ENVISAT sensors, to further consider the most recent ones, such as COSMO-SkyMed, Sentinel-1 and SAOCOM-1, which allow notable improvements in the investigation and monitoring of the detected displacements. The final part of the presentation will be devoted to describing some possible, future trends of the DInSAR scenario.